Proc. Natl. Acad. Sci. USA
Vol. 90, pp. 6320–6324, July 1993
Biochemistry

Crystal structure of human immunodeficiency virus type 1 reverse transcriptase complexed with double-stranded DNA at 3.0 Å resolution shows bent DNA

ALFREDO JACOBO-MOLINA*, JIANPING DING*, RAYMOND G. NANNI*, ARTHUR D. CLARK, JR.*, XIAODE LU*, CHRIS TANTILLO*, ROGER L. WILLIAMS*, GREG KAMER*†, ANDREA L. FERRIS‡, PATRICK CLARK§, AMNON HIZI¶, STEPHEN H. HUGHES‡, AND EDWARD ARNOLD*‖

*Center for Advanced Biotechnology and Medicine and Chemistry Department, Rutgers University, Piscataway, NJ 08854-5638; †Kamer Crystallographic Software, West Lafayette, IN 47906-4511; §Program Resources, Inc., and ‡Advanced BioScience Laboratories–Basic Research Program, National Cancer Institute–Frederick Cancer Research and Development Center, Frederick, MD 21702-1201; and ¶Department of Cell Biology and Histology, Sackler School of Medicine, Tel Aviv University, Tel Aviv, Israel 69778

Communicated by Aaron J. Shatkin, March 31, 1993 (received for review January 12, 1993)

ABSTRACT **The crystal structure of a ternary complex of human immunodeficiency virus type 1 reverse transcriptase (HIV-1 RT) heterodimer (p66/p51), a 19-base/18-base double-stranded DNA template-primer, and a monoclonal antibody Fab fragment has been determined at 3.0 Å resolution. The four individual subdomains of RT that make up the polymerase domains of p66 and p51 are named fingers, palm, thumb, and connection [Kohlstaedt, L. A., Wang, J., Friedman, J. M., Rice, P. A. & Steitz, T. A. (1992) *Science* 256, 1783–1790]. The overall folding of the subdomains is similar in p66 and p51 but the spatial arrangements of the subdomains are dramatically different. The template-primer has A-form and B-form regions separated by a significant bend (40–45°). The most numerous nucleic acid interactions with protein occur primarily along the sugar-phosphate backbone of the DNA and involve amino acid residues of the palm, thumb, and fingers of p66. Highly conserved regions are located in the p66 palm near the polymerase active site. These structural elements, together with two α-helices of the thumb of p66, act as a clamp to position the template-primer relative to the polymerase active site. The 3′-hydroxyl of the primer terminus is close to the catalytically essential Asp-110, Asp-185, and Asp-186 residues at the active site and is in a position for nucleophilic attack on the α-phosphate of an incoming nucleoside triphosphate. The structure of the HIV-1 RT/DNA/Fab complex should aid our understanding of general mechanisms of nucleic acid polymerization. AIDS therapies may be enhanced by a fuller understanding of drug inhibition and resistance emerging from these studies.**

In retroviruses such as the human immunodeficiency virus type 1 (HIV-1), reverse transcriptase (RT) is the sole enzyme necessary for the catalytic transformation of single-stranded viral RNA into the double-stranded linear DNA that is integrated into host cell chromosomes. HIV-1 RT is composed of two subunits of 66 kDa and 51 kDa (p66 and p51) (reviewed in refs. 1 and 2). The N-terminal 440 amino acids of p66 constitute the polymerase domain and the C-terminal 120 amino acids comprise the RNase H domain. The p51 subunit of HIV-1 RT corresponds to the polymerase domain of the p66 subunit. HIV-1 RT is the target for 3′-azido-3′ deoxythymidine (AZT), dideoxyinosine (ddI), and dideoxycytidine (ddC), the only drugs currently approved for treating HIV-1 infections. Although these drugs are widely used, each has serious side effects, which include toxicity and the rapid emergence of resistant strains of virus (3, 4). Numerous nonnucleoside compounds—e.g., the TIBO compounds {tetrahydro-imidazo[4,5,1-jk][1,4]-benzodiazepin-2(1H)-one and -thione derivatives} (5) and nevirapine (6)—are effective inhibitors of HIV-1 RT. However, strains of virus resistant to these compounds also arise rapidly (7). The mutations that confer resistance to nucleoside and nonnucleoside inhibitors are located in the polymerase domain of HIV-1 RT. The high-resolution structure of HIV-1 RT should accelerate the design of new and improved inhibitors.

A 3.5 Å resolution structure of HIV-1 RT complexed with the nonnucleoside inhibitor nevirapine has been reported (8). Although the resolution of the study was not sufficient to determine the position of every amino acid and their side chains, the overall folding of the enzyme was described.

We have prepared crystals of a ternary complex (9) of the HIV-1 RT p66/p51 heterodimer, a double-stranded DNA (dsDNA) template-primer, and the antigen-binding fragment (Fab fragment) of a noninhibiting antibody that diffract x-rays to 2.8 Å resolution, and reported the structure of this complex at 7 Å resolution (10). At this resolution it was possible to determine the location of the template-primer and the relative positions of the polymerase and the RNase H active sites. In addition, it was shown that when the nucleic acid substrate was bound to RT a significant portion of the protein moved out of the nucleic acid-binding site.

Here we report the structure of the RT–dsDNA–Fab28 complex at 3.0 Å resolution. The overall arrangement of the enzyme is similar to that previously reported (8). The template-primer binds to RT in a catalytically relevant fashion. The primer 3′-OH is positioned close to the polymerase active site, and the most numerous contacts between the enzyme and the DNA occur in the p66 palm, thumb, and fingers subdomains. The nucleic acid is an A-form/B-form DNA hybrid that has a bend of 40–45° at the junction of the A-form and B-form regions.**

MATERIALS AND METHODS

Crystal Treatment and Data Collection. Crystallization, low-resolution data collection, and procedures used for isomorphous heavy atom phasing and refinement have been de-

The publication costs of this article were defrayed in part by page charge payment. This article must therefore be hereby marked "*advertisement*" in accordance with 18 U.S.C. §1734 solely to indicate this fact.

Abbreviations: HIV-1, human immunodeficiency virus type 1; RT, reverse transcriptase; MIR, multiple isomorphous replacement; dsDNA, double-stranded DNA; CHESS, Cornell High Energy Synchrotron Source.

‖To whom reprint requests should be addressed at: Center for Advanced Biotechnology and Medicine (CABM), Rutgers University Chemistry Department, 679 Hoes Lane, Piscataway, NJ 08854-5638.

**The Cα coordinates of the HIV-1 RT heterodimer and the phosphorus coordinates of the template-primer have been deposited in the Protein Data Bank, Chemistry Department, Brookhaven National Laboratory, Upton, NY 11973 (Entry 1HMI).

scribed (9, 10). The crystals of the ternary complex of HIV-1 RT–dsDNA–Fab28 belong to the space group $P3_212$ with unit cell dimensions of $a = 169.0$, $c = 221.0$ Å. The asymmetric unit contains one complex with a molecular mass of 180 kDa. Table 1 summarizes the statistics of the MIR phasing calculations to 3.0 Å resolution. Crystals were transferred to 20-μl hanging drops containing 100 mM sodium cacodylate (pH 5.6), 63% saturated ammonium sulfate (wt/vol), 18% glycerol (vol/vol), and 0.1 mM of the 19/18 DNA (the sequence of the 19-mer strand is 5′-ATGGCGCCCGAACAGGGAC-3′, where the 5′-A forms the one-base overhang in the 19/18 DNA) 2–8 hr at 4°C before mounting. X-ray diffraction datasets from CHESS were collected using the F1 beamline ($\lambda = 0.91$ Å) and measurements were merged from multiple crystals (MTOPS package used for processing and scaling; G.K. and E.A., unpublished). Exposure times were usually 6–8 sec for storage phosphor image plates and 16–24 sec for Kodak DEF x-ray film. The effective resolution of image plate data (using Fuji image plates) was 0.5 Å better than film.

Electron Density Map Calculations. The combination of all area detector and synchrotron data (2 native and 12 derivative datasets; some of the calculations used a total of 21 derivative datasets) produced the best electron density maps from MIR/solvent flattening calculations. The datasets were merged using local scaling by resolution ranges with the CHESS glycerol native dataset as reference (11). The parameters used for automatic mask generation during solvent flattening (12) at 3.0 Å were solvent fraction = 60–75%, empirical constant S = 0.60, and radius = 8 Å (PHASES package††).

Model Building into Electron Density. Secondary structural elements of HIV-1 RT were identified using a number of electron density maps with resolution limits between 3.0 and 4.0 Å; assignment of some of the connections was facilitated by the reported structure of HIV-1 RT complexed with nevirapine (8). The atomic model has been constructed using program O (13). The amino acid residues in most regions of HIV-1 RT have been assigned with confidence. However, residue assignments are less certain owing to weak or ambiguous electron density in some segments of the thumb and connection subdomains of p66 and p51. Regions with the weakest density (correlation coefficient < 0.2 for two or more consecutive residues using the electron density map shown in Fig. 1 and the real space fit routine in program O) are p66 residues 68–73, 245–252, 277–279, 285–287, 296–297, and 554–556 and p51 residues 89–91, 102–103, 244–245, 248–250, 277–278, 299–300, and 357–361. RNase H modeling was initially based on the HIV-1 RNase H coordinates of Davies *et al.* (14), with subsequent adjustments of loops and side chain orientations. The loop connecting residues 537–543, which was not ordered in the structure of Davies *et al.* (14), is ordered in the structure reported here. The most prominent electron density for the DNA corresponds to the sugar-phosphate backbone. One strategy for building the DNA used fitting of either A- or B-form nucleotides. Another approach used optimized phosphorus positions and positioning of idealized Watson–Crick base pairs. There is good electron density for the primer terminus and the one-base adenine overhang of the template strand. At the blunt end of the duplex, the electron density for the last base pair is relatively poor. Interpretation of the Fab28 structure was initially guided by using the four β-barrel domains of McPC603 (15). The Fab28 model has been completed based on the sequence of Fab28 (A.L.F. and S.H.H., unpublished).

RESULTS AND DISCUSSION

Structure of HIV-1 RT. The polymerase domains of p66 and p51 each contain four subdomains, denoted fingers, palm, thumb, and connection (8). Although the structures of the subdomains within p66 and p51 are similar, the relative arrangement of the four subdomains within the two subunits is different. A representative portion of the current atomic model in a 3.0 Å resolution electron density map is shown in Fig. 1. The overall folding of p66 and p51 is shown in Fig. 2. As expected, the structure of HIV-1 RT in our ternary complex resembles that of HIV-1 RT complexed with nevirapine. However, the precise location of some secondary structural elements, in particular those involved in interactions with the nucleic acid substrate and the Fab, may be different between the two structures. For instance, the p51 polypeptide backbone position corresponding to β11b, β12, β13, and β14 in p66 was uncertain in the RT/nevirapine complex and is ordered in the structure reported here. This could be due in part to the fact that Fab28 is bound to p51 at the region corresponding to β11b-β12 in p66.

The template-primer binds in a large cleft formed by the fingers, palm, and thumb of p66. The connection subdomains of p66 and p51 and the p51 thumb make up much of the "floor" of the template-primer binding cleft; however, there are few contacts between the DNA and the floor of the cleft. Strand β18 of p66 interacts with the template and the primer. Helix αL of p51 makes contact with the primer strand, and β20 of p51 makes contact with the template strand; these may be the only close interactions between p51 and the DNA.

The distance between the polymerization and RNase H active sites, as measured by the dsDNA in the complex, is 17 or 18 nucleotides. Biochemical estimates of the separation using an RNA/DNA substrate have ranged from 7 to 19

Table 1. Data used in and phasing statistics of the structure determination at 3.0 Å resolution

Dataset	Resolution limit,* Å	R_{merge}†	R_{deriv}‡	Unique reflections	Phasing power§¶
Native	2.8	0.13		76,903	88.1%
Hg-dUTP	3.0	0.13	0.18	46,417	1.39
Hg-UTP1	3.0	0.12	0.18	44,559	1.37
Hg-UTP2	3.0	0.12	0.18	50,263	1.52
PCMBS	3.0	0.14	0.17	57,855	1.36
PIP1	4.0	0.13	0.25	18,822	1.14
PIP2	3.5	0.13	0.20	34,395	0.60
TAMM	3.5	0.13	0.16	38,456	1.42
Native	5.9	0.06		7,654	83.0%
$HgCl_2$	6.5	0.06	0.18	4,430	1.38
Hg-dUTP	5.9	0.05	0.15	5,478	2.04
MePhHg	6.5	0.07	0.15	3,846	1.43
PIP	6.5	0.07	0.21	3,485	1.55
TAMM	6.0	0.04	0.14	3,942	1.71

The abbreviations for the heavy atoms are as follows: Hg-dUTP, 5-mercurideoxyuridine 5′-triphosphate; Hg-UTP, 5-mercuriuridine 5′-triphosphate; MePhHg, methyl phenyl mercury; PCMBS, *p*-chloromercuribenzene sulfonate; PIP, di-μ-iodobis(ethylenediamine)-diplatinum (II) nitrate; and TAMM, tetrakis(acetoxymercuri)methane. The heavy atom positions are related to those detailed in the 7 Å resolution structure determination (10). The overall multiple isomorphous replacement (MIR) figure of merit (FOM) is 0.490 for 66,059 reflections to 3 Å resolution and 0.846 after solvent flattening (S = 60%). The MIR FOM for shells containing 13,210 reflections as a function of resolution are as follows: (mean FOM, resolution) (0.70, 7.6 Å; 0.60, 4.6 Å; 0.49, 3.9 Å; 0.37, 3.4 Å; 0.29, 3.1 Å).

*Datasets with resolution limits 5.9 Å and below were collected using a Xuong-Hamlin Mark II multiwire area detector in the Center for Advanced Biotechnology and Medicine/Waksman Biomolecular Crystallography Laboratory. All higher resolution datasets were collected at the Cornell High Energy Synchrotron Source (CHESS).

†$R_{merge} = \Sigma |I_{obs} - \langle I \rangle| / \Sigma \langle I \rangle$.

‡$R_{deriv} = \Sigma |F_{PH} - F_P| / \Sigma F_P$.

§Phasing power = $[\Sigma |F_H|^2 / \Sigma (|F_{PH,obs}| - |F_{PH,calc}|)^2]^{1/2}$.

¶For native datasets, this column lists the completeness of data to the resolution limit given.

††Furey, W. & Swaminathan, S., American Crystallography Association Meeting, April, 1990, New Orleans, p. 73 (abstr. PA33).

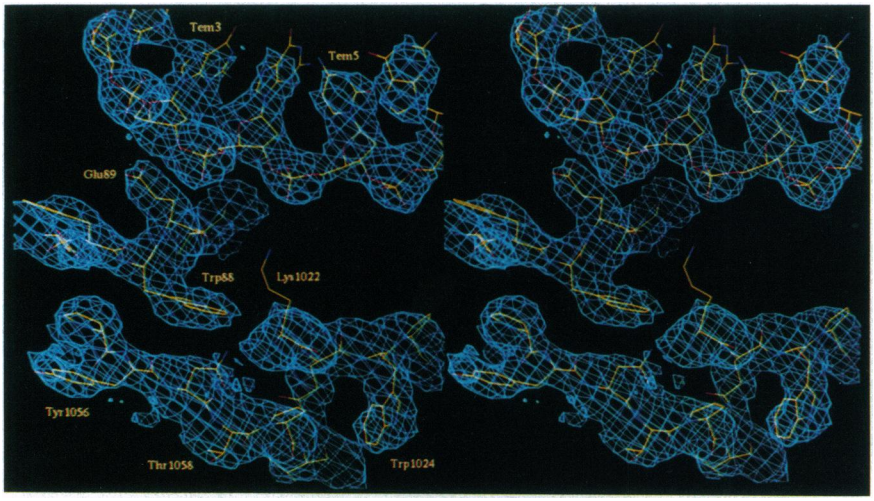

FIG. 1. Atomic model in a 3.0 Å resolution electron density map. Labeled are residues Trp-88 and Glu-89 [the site of ddGTP-resistant mutation (16), shown interacting with the template strand] in p66, Lys-22, Trp-24, Tyr-56, and Thr-58 in p51 (numbered 1022, 1024, etc., to distinguish from the corresponding residues in p66), and the template nucleotides Tem3 and Tem5. Sixteen cycles of solvent flattening starting with MIR phases from 12 derivatives (see Table 1) combined with those from a partial atomic model refined using XPLOR (17) [20 cycles of positional refinement, 10,759 of 12,200 possible nonhydrogen atoms; $R = 0.316$ for 62,339 reflections with $F > 3\sigma(F)$ to 3.0 Å resolution] yielded a molecular envelope and phases that were then input for 12 cycles of iterative phase extension. During these final 12 cycles, the combination used only the MIR phases, greatly reducing model bias.

nucleotides (19–22). Our previous measurements of 15 or 16 nucleotides used a straight B-DNA model as reference (10) and not the actual bent A/B DNA hybrid (see below).

Relative to its position in p66, the thumb of p51 is moved away from the palm and makes significant contacts with RNase H. The connection subdomain of p51 is folded up onto the palm of p51 between the fingers and the thumb. As a consequence, p51 does not have a DNA-binding cleft. This is consistent with the observation that in the heterodimer, p51 has no polymerase activity (23, 24). We reported earlier that there was substantial electron density in the DNA-binding groove of RT in HIV-1 RT/Fab28 crystals that did not contain DNA (10). This density has now been identified as the p66 thumb, indicating that this is a flexible element in the structure. The p66 thumb is in an upright position in the DNA-containing structure reported here and in the complex with nevirapine (8), suggesting that the binding of nevirapine affects the position of the thumb, and potentially, its mobility.

RNase H Domain in the HIV-1 RT–dsDNA Complex. Although there are minor differences, the structure of RNase H conforms well to the structure of the free RNase H domain (14). The portions of RNase H containing amino acids that have

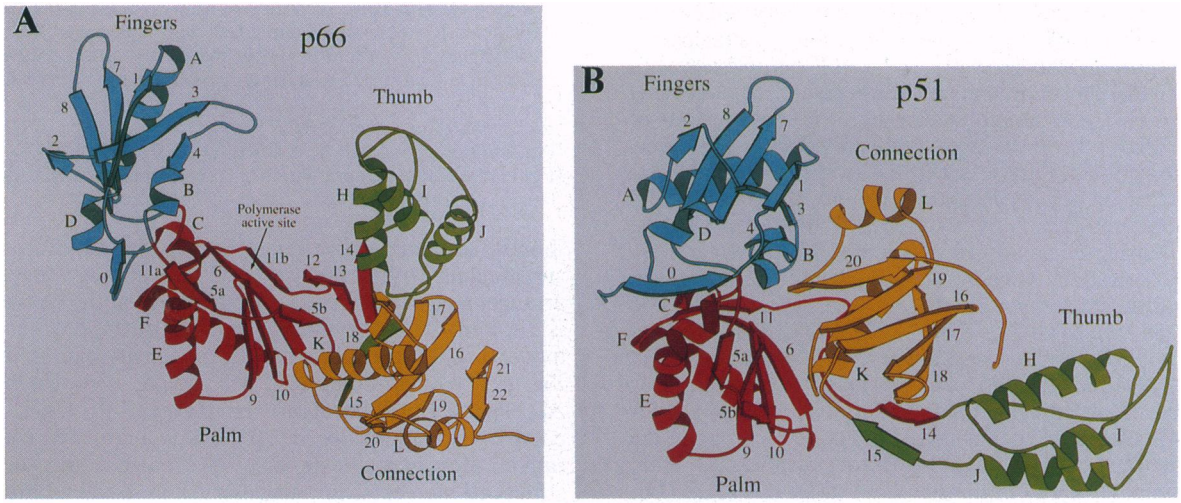

SS	p66	p51	SS	p66	p51	SS	p66	p51	SS	p66	p51	SS	p66
β0	7-12	1007-1012	β6	105-112	1105-1111	β11a	214-217	1214-1219	β16	326-333	1325-1333	β1'	438-447
β1	18-24	1019-1022	αC	114-117	1112-1115	β11b	219-222	----------	β17	336-341	1336-1343	β2'	452-459
αA	28-44	1028-1044	αD	122-127	1122-1127	β12	227-229	----------	β18	350-358	1350-1358	β3'	462-470
β2	49-51	1049-1051	β7	128-134	1128-1134	β13	232-235	----------	αK	364-382	1364-1381	αA'	474-488
β3	56-63	1056-1063	β8	141-147	1141-1147	β14	238-242	1239-1242	β19	388-391	1386-1392	β4'	492-497
β4	73-77	1072-1076	αE	155-174	1155-1174	αH	255-268	1254-1270	αL	395-404	1395-1404	αB'	500-508
αB	78-83	1078-1084	β9	178-183	1179-1183	αI	278-286	1277-1283	β20	408-412	1410-1416	αD'	516-527
β5a	86-90	1087-1090	β10	186-191	1186-1191	αJ	298-311	1298-1310	β21	421-424	----------	β5'	530-536
β5b	94-96	1094-1096	αF	195-212	1198-1212	β15	316-321	1316-1319	β22	427-430	----------	αE'	544-555

FIG. 2. Folding diagrams generated using MOLSCRIPT (18) showing arrangement of secondary structural elements within the p66 (*A*) and p51 polymerase (*B*) domains of HIV-1 RT. Spirals represent α-helices and arrows represent β-strands. Enumeration of secondary structural elements and naming and coloring of the subdomains of the polymerase domains as fingers (cyan), palm (red), thumb (green), and connection (yellow) follow the conventions used in the description of HIV-1 RT complexed with nevirapine (8). The boundaries defining the secondary structural elements (named in the SS columns, largely defined using routine YASSPA of program O) are listed below the diagrams, including those for the RNase H domain, which is not shown. Residue numbers in p51 have 1000 added to distinguish from corresponding residues in p66. For consistency, the secondary structural elements assigned to each subdomain were kept as proposed before (8). The main structural differences between the reported RT/nevirapine complex and the RT/DNA/Fab complex reported here are (*i*) β0, β5a, β11a, β21, and β22 are additional β-strands in p66 and β0 and β5a are additional β-strands in p51; (*ii*) strand β5a appears to be part of αB in the RT/nevirapine complex; (*iii*) β5b in p66 and p51 and β11b in p66 in our structure may correspond to β5 and β11, respectively, in the RT/nevirapine complex; (*iv*) the region between β11a and the thumb of p51 is ordered in our structure; and (*v*) the electron density corresponding to helix G in the RT/nevirapine complex is weak in p66 and p51 in our structure, not currently permitting a clear secondary structure assignment.

potential interactions with the DNA include αA, αB, the β1–β2 hairpin [using the RNase H nomenclature of Davies *et al.* (14)], and the loop containing His-539. dsDNA is not used as a substrate by the RNase H of HIV-1 RT and the template strand in the complex is not in a position that is favorable for cleavage by RNase H. The composition of the template-primer, and consequently its structure, could regulate RNase H activity.

Structure of the dsDNA Template-Primer in the Complex with HIV-1 RT. The structure of HIV-1 RT complexed with the 19/18 DNA template-primer is shown in Fig. 3. The DNA in the crystals is a template-primer composed of oligonucleotides of 19 and 18 bases (10). We have used Tem and Pri to designate positions in the template and primer strands, respectively. The positions are numbered from 5′ to 3′. The template-primer conforms more closely in structure to classical A-form DNA near the polymerase active site and to B-form DNA near the RNase H active site. RNA/RNA and RNA/DNA duplexes, which are expected to adopt an A-form conformation (28), are used as template-primers during retroviral reverse transcription. Because RT must be able to use these template-primers it may induce the DNA/DNA duplex to adopt a similar conformation. There is a significant bend in the DNA duplex such that the helical axes of the A-form and B-form portions make an angle of about 40–45° (Fig. 3*A*). The bend is distributed over approximately four nucleotides and occurs in the vicinity of contacts with helix αH of the p66 thumb (Fig. 3*B*). A modeling study of an A- to B-form DNA transition predicted a DNA bend of 26° at the A/B junction (29). Bending of the template-primer may have functional implications for RT catalysis, translocation, fidelity, and/or processivity. It will be interesting to see if a similar bend occurs with different template-primers or with other polymerases.

Contacts Between HIV-1 RT and the dsDNA Template-Primer. The most extensive contacts between DNA and protein involve the sugar-phosphate backbone of the nucleic acid and the palm, thumb, and fingers subdomains of p66 (Fig. 3*B*). The p66 palm contains the polymerase active site that is defined by a triad of aspartic acid residues at positions 110, 185, and 186. These amino acids may bind the divalent cations that are required for catalysis. The 3′-OH of the primer terminus is close to the catalytic triad (Fig. 4) and is appropriately positioned for nucleophilic attack on the α-phosphate of an incoming nucleoside triphosphate. In support of this interpretation, a mercurated nucleoside triphosphate binds at precisely this site (10). As shown in Fig. 3*B*, the regions surrounding the polymerase active site correspond to motifs that are conserved in polymerases (26, 27). This region of the

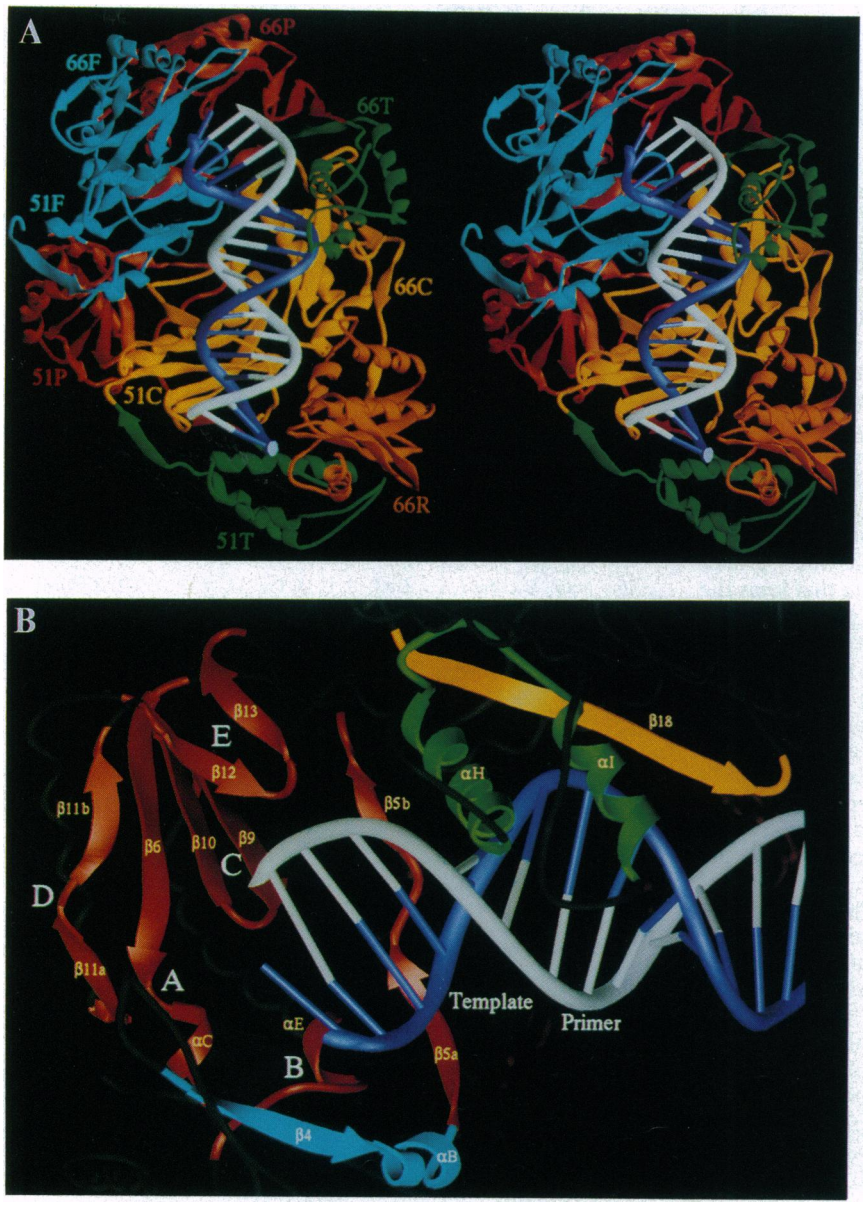

FIG. 3. Interactions of HIV-1 RT with dsDNA represented using program RIBBONS (25). (*A*) Stereo ribbon diagram of the HIV-1 RT p66/p51 heterodimer with 19/18 DNA template-primer bound showing the bend in the DNA and the interactions between the DNA and HIV-1 RT. The view is from above the template-primer binding cleft. The protein subdomains of the p66 and p51 polymerase domains are colored as in Fig. 2, and RNase H is colored orange; the subdomain labels indicate subunit and subdomain (e.g., 66T corresponds to the p66 thumb and 51F corresponds to the p51 fingers). The primer strand is shown in white and the template strand is shown in blue. The bars connecting the complementary positions along the two strands represent the approximate locations of the base pairs. The complex is oriented with the p66 polymerase active site toward the top of the figure. The dsDNA bends significantly in the vicinity of its interaction with helix H of the p66 thumb. Helix H is partially embedded in the minor groove of the DNA. The connection subdomains of p66 and p51 form a considerable fraction of the floor of the binding cleft. There are relatively few interactions between RT and the DNA away from the polymerase active site region. (*B*) Structural elements near the HIV-1 RT polymerase active site that make potential contacts with the DNA and those corresponding to conserved motifs are shown and the secondary structural units are labeled. The approximate positions of conserved sequence motifs found in all RNA-dependent polymerases (26, 27) are indicated as A–E. The conserved motifs appear to contain elements that participate directly in nucleoside triphosphate binding and catalysis (A, C, and perhaps D) and elements that are involved in the precise positioning of the template-primer relative to the active site (B and E). This entire apparatus, together with helices αH and α1 of the p66 thumb, could participate in translocation of the template-primer following nucleotide incorporation.

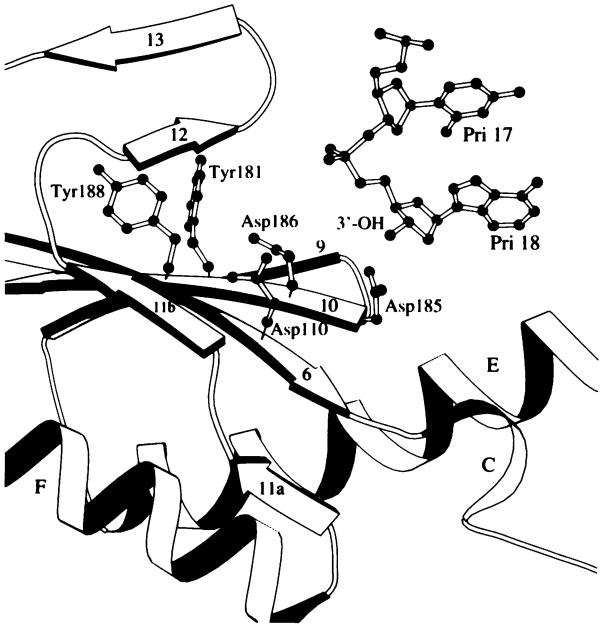

FIG. 4. Structure of the polymerase active site of HIV-1 RT [generated using MOLSCRIPT (18)], highlighting the relative positions of the "catalytic triad" (Asp-110, Asp-185, and Asp-186) and the 3'-terminal nucleotides of the primer strand. Selected secondary structural elements of the p66 palm subdomain are indicated with spirals for α-helices and arrows for β-strands. The locations of the catalytically essential Asp-110, Asp-185, and Asp-186 residues of p66 are shown relative to the primer terminus of the DNA. Also shown are Tyr-181 and Tyr-188, which are important components of the binding pocket for nonnucleoside inhibitors of HIV-1 RT (7, 8).

palm of p66 has considerable structural similarity to the polymerase active site of the Klenow fragment of *Escherichia coli* DNA polymerase I (8, 30), suggesting that these polymerases diverged from a common ancestor and that other polymerases will make similar contacts with nucleic acids in this region. As noted earlier (8) and unambiguously defined by this study, the orientation of nucleic acid synthesis by Klenow fragment is opposite to that originally proposed (30).

The palm and thumb of p66 appear to act together as a clamp that positions the template-primer relative to the polymerase active site. We have designated the β12-β13 hairpin, which is close to the nevirapine-binding pocket (8), as the "primer grip" because of its proximity to the phosphate that joins the nucleotides at the primer terminus (i.e., the phosphodiester linkage between Pri17 and Pri18, Fig. 4). The "template grip" consists of portions of the p66 palm and fingers that are closely associated with nucleotides of the template strand. These include β4 and αB of the fingers (near Tem1, Tem2, and Tem3), the β8-αE connecting loop (near Tem1 and Tem2), and β5a of the palm (near Tem3 and Tem4). Kohlstaedt *et al.* (8) suggested that the p66 fingers might be involved in binding the template. We have built models with extended templates that strongly suggest that the p66 fingers, in particular β4 and the β3-β4 loop, position a longer template strand.

The αH helix of the p66 thumb makes contacts with the sugar-phosphate backbone of the primer strand. The adjacent antiparallel helix αI makes contacts with the sugar-phosphate backbone of the template strand. These helices may function as tracks over which the template-primer moves during translocation (Fig. 3*B*). Although the thumbs of Klenow fragment (30) and T7 RNA polymerase (‡‡) are not strictly homologous to the thumb of HIV-1 RT, they do contain analogous antiparallel structural elements, suggesting that most nucleotide polymerases use this type of structure for binding and translocation of template-primer.

‡‡Sousa, R., Rose, J., Chung, Y. J. & Wang, B. C., American Crystallography Association Meeting, August, 1992, Pittsburgh, p. 62 (abstr. BB03).

We thank Aaron Shatkin, Helen Berman, and Gail Ferstandig Arnold for careful reading of the paper, Paul Boyer, Brad Preston, Koen Andries, Paul Janssen, and Marvin Cassman for valuable discussions and encouragement, Helen Berman, R. Srinivasan, Jaroslav Vojtechovsky, and Wilma Olson for advice about DNA model building, Wanyi Zhang for model evaluation, and Don Bilderback and Steve Ealick for support of data collection at CHESS. This work was supported by grants from the National Institutes of Health (AI 27690), Center for Advanced Biotechnology and Medicine, Janssen Research Foundation, and Johnson & Johnson to E.A., a grant from the American Foundation for AIDS Research to A.J.-M., and contracts from the National Cancer Institute and National Institute of General Medical Sciences to S.H.H.

1. Goff, S. P. (1990) *J. Acquired Immune Defic. Syndr.* **3**, 817–831.
2. Jacobo-Molina, A. & Arnold, E. (1991) *Biochemistry* **30**, 6351–6361.
3. Larder, B. A. & Kemp, S. D. (1989) *Science* **246**, 1155–1158.
4. St. Clair, M. H., Martin, J. L., Tudor-Williams, G., Bach, M. C., Vavro, C. L., King, D. M., Kellam, P., Kemp, S. D. & Larder, B. A. (1991) *Science* **253**, 1557–1559.
5. Pauwels, R., Andries, K., Desmyter, J., Schols, D., Kukla, M. J., Breslin, H. J., Raeymaeckers, A., Van Gelder, J., Woestenborghs, R., Heykants, J., Schellekens, K., Janssen, M. A. C., De Clercq, E. & Janssen, P. A. J. (1990) *Nature (London)* **343**, 470–474.
6. Merluzzi, V. J., Hargrave, K. D., Labadia, M., Grozinger, K., Skoog, M., Wu, J. C., Shih, C.-K., Eckner, K., Hattox, S., Adams, J., Rosenthal, A. S., Faanes, R., Eckner, R. J., Koup, R. A. & Sullivan, J. L. (1990) *Science* **250**, 1411–1413.
7. Nunberg, J. H., Schleif, W. A., Boots, E. J., O'Brien, J. A., Quintero, J. C., Hoffman, J. M., Emini, E. A. & Goldman, M. E. (1991) *J. Virol.* **65**, 4887–4892.
8. Kohlstaedt, L. A., Wang, J., Friedman, J. M., Rice, P. A. & Steitz, T. A. (1992) *Science* **256**, 1783–1790.
9. Jacobo-Molina, A., Clark, A. D., Jr., Williams, R. L., Nanni, R. G., Clark, P., Ferris, A. L., Hughes, S. H. & Arnold, E. (1991) *Proc. Natl. Acad. Sci. USA* **88**, 10895–10899.
10. Arnold, E., Jacobo-Molina, A., Nanni, R. G., Williams, R. L., Lu, X., Ding, J., Clark, A. D., Jr., Zhang, A., Ferris, A. L., Clark, P., Hizi, A. & Hughes, S. H. (1992) *Nature (London)* **357**, 85–89.
11. Matthews, B. W. & Czerwinski, E. W. (1975) *Acta Crystallogr. Sect. A* **31**, 480–487.
12. Wang, B. C. (1985) *Methods Enzymol.* **115**, 90–112.
13. Jones, T. A., Zou, J. Y., Cowan, S. W. & Kjeldgaard, M. (1991) *Acta Crystallogr. Sect. A* **47**, 110–119.
14. Davies, J. F., Hostomska, Z., Hostomsky, Z., Jordan, S. R. & Matthews, D. A. (1991) *Science* **252**, 88–95.
15. Satow, Y., Cohen, G. H., Padlan, E. A. & Davies, D. R. (1986) *J. Mol. Biol.* **190**, 593–604.
16. Song, Q., Yang, G., Goff, S. P. & Prasad, V. R. (1992) *J. Virol.* **66**, 7568–7571.
17. Brunger, A. T. (1992) XPLOR program manual (Yale Univ., New Haven, CT), Version 3.0.
18. Kraulis, P. J. (1991) *J. Appl. Crystrallogr.* **24**, 946–950.
19. Wohrl, B. M. & Moelling, K. (1990) *Biochemistry* **29**, 10141–10147.
20. Schatz, O., Mous, J. & Le Grice, S. F. J. (1990) *EMBO J.* **9**, 1171–1176.
21. Furfine, E. S. & Reardon, J. E. (1991) *Biochemistry* **30**, 7041–7046.
22. Gopalakrishnan, V., Peliska, J. A. & Benkovic, S. J. (1992) *Proc. Natl. Acad. Sci. USA* **89**, 10763–10767.
23. LeGrice, S. F. J., Naas, T., Wohlgensinger, B. & Schatz, O. (1991) *EMBO J.* **10**, 3905–3911.
24. Hostomsky, Z., Hostomska, Z., Fu, T.-B. & Taylor, J. (1992) *J. Virol.* **66**, 3179–3182.
25. Carson, M. (1987) *J. Mol. Graphics* **5**, 103–106.
26. Poch, O., Sauvaget, I., Delarue, M. & Tordo, N. (1989) *EMBO J.* **8**, 3867–3874.
27. Delarue, M., Poch, O., Tordo, N., Moras, D. & Argos, P. (1990) *Protein Eng.* **6**, 461–467.
28. Kornberg, A. & Baker, T. A. (1991) *DNA Replication* (Freeman, New York), 2nd Ed., pp. 931.
29. Selsing, E., Wells, R. D., Alden, C. J. & Arnott, S. (1979) *J. Biol. Chem.* **254**, 5417–5422.
30. Ollis, D. L., Brick, P., Hamlin, R., Xuong, N. G. & Steitz, T. A. (1985) *Nature (London)* **313**, 762–766.